Available online at www.sciencedirect.com
SCIENCE DIRECT®
ELSEVIER
International Journal of Multiphase Flow 31 (2005) 393–415
International Journal of Multiphase Flow
www.elsevier.com/locate/ijmulflow

Heat transfer characteristics of water and APG surfactant solution in a micro-channel heat sink

D. Klein, G. Hetsroni *, A. Mosyak

Department of Mechanical Engineering, Technion—Israel Institute of Technology, Haifa 32000, Israel

Received 11 April 2004; received in revised form 25 January 2005

Abstract

The steady increase in internal heat production of cost and high performance electronic components has lead researchers to seek improved ways to remove the heat generated. Single-phase liquid flow has been considered as a potential solution for solving this cooling problem. However, when considering that any solution needs to be of low cost and low mass fluxes and yet retain low temperature gradients across the electronic components, it seems that two-phase boiling flow is preferred. Surfactant solutions have been introduced in connection with enhancement of the boiling processes. We investigated the effects of surfactant solution flows through a micro-channel heat sink. The experimental setup included a high-speed IR radiometer and a CCD camera that were used to characterize the test module. The module consisted of inlet and outlet manifolds that distributed surfactant solutions through an array of 26 parallel micro-channels. The experimental results have shown that there exists an optimal solution concentration and mass flux for enhancing heat removal. Surfactant solution boiling flows were also found to stabilize the maximum and average surface temperatures for a wide range of applied heat fluxes. In addition, the use of surfactant solutions at low mass fluxes has led to CHF enhancement when compared to regular water flows. In the last part of this work, possible explanations for the observed non-ionic surfactant effects are presented.

Keywords: Micro-channels; Surfactants; Heat transfer; Flow regimes

* Corresponding author. Tel:. +972 4 8292058; fax: +972 4 8238101.
E-mail address: hetsroni@tx.technion.ac.il (G. Hetsroni).

0301-9322/$ - see front matter © 2005 Elsevier Ltd. All rights reserved.
doi:10.1016/j.ijmultiphaseflow.2005.01.007

1. Introduction

Micro-channel heat exchangers are devices, which enable liquid flow through parallel channels having a hydraulic diameter of 10–1000 μm. These devices are ideally suited for high heat flux dissipation from small surface areas in a broad range of high performance electronics, power devices, electric vehicles and advanced military avionics. Air is the most affordable working fluid, and remains the most widely used coolant for most applications. However, the poor thermal transport properties of air greatly limits its cooling potential to relatively low heat flux devices. Better results are possible with fluorochemical liquids, while the most demanding cooling situations are typically managed with water. Superior performances require a change-of-phase (boiling) of the liquid coolant.

Numerous correlations have been proposed in the literature for heat transfer, based on experimental investigations on liquid and gas flow in micro-channels. Sobhan and Garimella (2001) presented a comprehensive review of these investigations in the past decade.

Experimental studies have shown a departure from the conventional theory for heat transfer. Choi et al. (1991) found that the measured Nusselt number in laminar flows exhibits a Reynolds number dependence, in contrast to the conventional prediction for fully developed laminar flows, in which the Nusselt number is constant. The heat transfer at forced convection in channels with a cross-section of 0.6×0.7 mm was experimentally investigated by Peng and Wang (1993). They showed that the dependence of the Nusselt number on the Reynolds number exhibited an unusual tendency. Weisberg et al. (1992) and Bowers and Mudawar (1994), also noted that the behavior of fluid flow and heat transfer in micro-channels without phase change is substantially different from that which typically occurs in conventionally sized channels. Wang and Peng (1994) reported single-phase heat transfer coefficients in six rectangular channels having $0.31 < d_h < 0.75$ mm for water and methanol. The Nusselt numbers were only 35% of those predicted by the Dittus–Boetler equation. However, Webb and Zhang (1998) found that their experimental results were adequately predicted by the commonly accepted correlations for single-phase flow in multiple tubes having hydraulic diameters between 0.96 and 2.1 mm. Wu and Little (1984) measured the flow and heat transfer characteristics for the flow of nitrogen gas in heat exchangers. The Nusselt numbers for laminar flow ($Re < 600$) were lower than those predicted by correlations. Peng and Peterson (1995) showed a strong effect of geometric configuration (aspect ratio and the ratio of the hydraulic diameter to the center-to-center distance of the micro-channels) on the heat transfer and flow characteristics in single-phase laminar flow. Zhang et al. (2002a) showed that addition of minute or high amounts of Triton X-100 surfactants to de-ionized water flowing through a 44 μm hydraulic diameter channel did not increase the single-phase heat transfer coefficient compared to regular de-ionized water.

Some authors provide experimental and numerical results for water flow in micro-channels in agreement with predicted values for the friction factor and Nusselt number. The experimental and numerical study of pressure drop and heat transfer in a single-phase micro-channel heat sink carried out by Qu and Mudawar (2002a,b) demonstrated that the conventional Navier–Stokes and energy equations can adequately predict the fluid flow and heat transfer characteristics of micro-channel heat sinks.

New questions have arisen in microscale flow and heat transfer. These problems have been considered in several review papers by Gad-el-Hak (1999), Mehendale et al. (1999) and Palm (2001).

The review by Gad-el-Hak (1999) focused on the physics related to the breakdown of the N–S equations. Mehendale et al. (1999) thought that since the heat transfer coefficients were based on the inlet and/or outlet fluid temperatures, not the bulk temperatures in almost all studies, comparison of conventional correlations is problematic. Palm (2001) also suggested several possible explanations for the variations of microscale single-phase heat transfer from the conventional theory, including surface roughness effects and entrance effects.

One drawback of a single-phase micro-channel heat exchanger is a relatively high temperature rise along the micro-channels compared to that for traditional heat sinks. Furthermore, the fluid flow rate might not be evenly distributed between the parallel micro-channels (Hetsroni et al., 2001a); therefore large spanwise gradients may occur as well. The gradients mentioned produce thermal stresses in elements and packages due to the differences in the coefficient of thermal expansion, thus undermining the devices' reliability. The same gradient undermines electrical reliability as well because of the dependence of an electronic component's mean time between failure (MTBF) on a component's temperature. These are two of the key reasons for seeking a nearly isothermal heat sink.

A two-phase micro-channel heat exchanger, which may achieve a uniform temperature profile of the heated surface, is an alternative method for decreasing temperature variations. Various aspects of change-of-phase heat transfer in micro-channels have been investigated recently by Peng and Wang (1998), Peng et al. (1998), Hetsroni et al. (2002a), Zhang et al. (2002a,b), Kandlikar (2002), Warrier et al. (2002), Qu and Mudawar (2003).

Hetsroni et al. (2002a) conducted experiments on flow boiling of a dielectric fluid Vertrel XF in a micro-channel heat exchanger. The heat exchanger had 21 parallel micro-channels with a base of 250 μm. The cooling fluid made it possible to maintain the temperature on the heated surface in the range 323–333 K with a heat flux up to 36 W/cm^2. The heat transfer coefficient was shown to increase with increasing thermodynamic equilibrium quality. Warrier et al. (2002) and Qu and Mudawar (2003) also observed an increase in the heat transfer coefficient with increasing thermodynamic equilibrium quality. Warrier et al. (2002) studied both single- phase forced convection, subcooled and saturated boiling in rectangular channels of a hydraulic diameter of 750 μm using FC-84 as the test fluid. In the range of vapor quality from 0.03 to 0.55, new correlations were proposed. Qu and Mudawar (2003) carried out experiments in a two-phase micro-channel heat sink containing 21 parallel channels having a 231×173 μm cross-section. The results revealed that the dominant heat transfer mechanism is forced convective boiling corresponding to annular flow. On the basis of a critical literature review and the work conducted by Kandlikar (2002), the following conclusions can be drawn: the heat transfer rate in multi-channel heat exchangers is different from that in single-channel heat exchangers. The effect of the inlet and outlet conditions, that is, manifolds material and their connection to parallel micro-channels was not studied.

It was shown by Hetsroni et al. (2001b, 2002b) that addition of minute amounts of surfactant additives to water significantly decreased the bubble size during pool boiling experiments. Under these conditions, the heat transfer coefficient increased in saturated boiling of surfactants compared to that in pure water. The surface tension force is important and might affect flow patterns and heat transfer in micro-channel heat exchangers. One study performed by Zhang et al. (2002a) revealed this phenomenon, yet their results did not show any potential improvement in heat transfer using Triton X-100 surfactant solutions. However, the intentional increase in surface cavities in a 72.5 μm hydraulic diameter micro-channel did improve the boiling heat transfer coefficient, which kept surface temperature stable under a wide range of applied heat fluxes.

In the present study, the working fluids were water and surfactant solutions that are safe in terms of environmental impact. Specifically, flow boiling at low values of mass fluxes was studied because it facilitated understanding of processes in micro-channel heat exchangers—utilizing small size pumps with small liquid flow rates. This paper emphasizes a number of points that seem to be of vital importance to the safety of industrial heat exchangers with small diameter channels and compares the performance of micro-channel heat exchangers using water as the working fluid to those using surfactant solutions. In addition, we aimed to determine the effect of dissolved gas on nucleation characteristics. Parallel triangular channels with common inlet and outlet manifolds were used. The experimental study is based on systematic observations and measurements by infrared radiometry and high-speed video images.

2. Experimental setup

We studied the heat transfer characteristics of single- and two-phase flows in a micro-channel heat sink (MCHS) for both water and surfactant solutions. The experimental facility was designed and constructed as illustrated schematically in Fig. 1.

2.1. Fluid flow system

The flow system contained a few elements: an entrance tank with a tap-regulated exit. A mini gear pump, producing flow rates up to 0.042 kg/s at a maximum pressure up to 145 kPa, at a con-

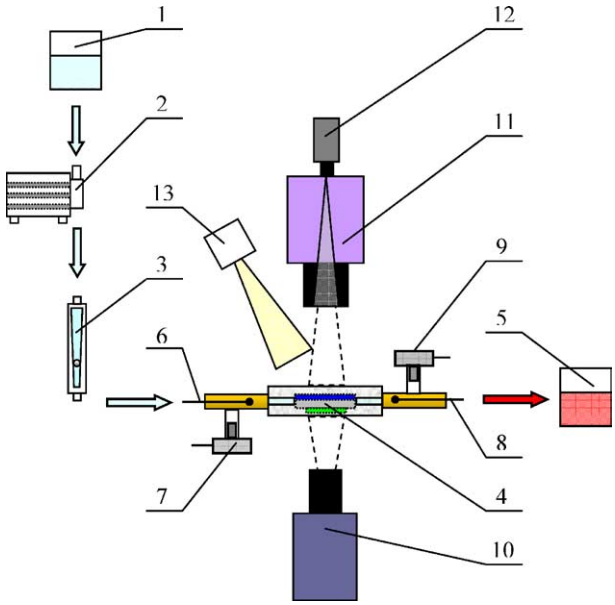

Fig. 1. Schematic side view of the experimental facility. 1—inlet tank, 2—mini-gear-pump, 3—rotameter, 4—test module, 5—exit tank, 6—inlet thermocouple, 7—inlet pressure gauge, 8—outlet thermocouple, 9—outlet pressure gauge, 10—high speed IR camera, 11—microscope, 12—high speed CCD camera, 13—external light source.

stant flow rate. A tubing of a 4.0 mm inner diameter delivered the pumped fluid into the test module and out to the exit tank. The experiments were performed in an open loop; therefore, the outlet pressure was close to atmospheric.

2.2. Test module

The micro-channel heat sink included two main components—test module and power supply unit. The test module consisted of inlet and outlet manifolds that were joined to the test chip and distributed the flow into and out of 26 parallel micro-channels. The Stainless Steel 416 "L" shaped manifolds are shown in Fig. 2. The tested chip with the heater is shown in Fig. 3. It was fabricated with a square shape 15×15 mm and 500 μm thick silicon $\langle 1\,0\,0 \rangle$ wafer, which was later bonded to a 530 μm thick Pyrex cover. On one side of the silicon wafer, 26 micro-channels were etched, with triangular shaped cross-sections, with a base $e = 210$ μm and a base angle of 54.7°. To prevent random local surface oxidation, the micro-channels were further treated to create a thin cover of silicon-oxide (a wetting surface). On the other side of the silicon wafer, a 9 μm thick aluminum heater was deposited. To enable soldering of connecting cables, a 1 μm copper layer was further deposited on the resistor pads. Given the deposition production process of the heater layers, most of the heat produced within the heater was transferred to the silicon chip with a very low thermal resistance and the rest to the surrounding by radiation and natural convection. The deposited serpentine pattern design allowed uniform heating over an area of 10×10 mm. The Pyrex cover was anodically bonded to the silicon chip, in order to seal the channels and enable fluid flow. The cover was transparent to 300–800 nm wavelengths and therefore enabled high-speed visualization of the two-phase flow regimes. The test chip was connected to the inlet and outlet manifolds by means of a specially mixed glue that was adjusted to the materials surface properties and expansion coefficients. In order to apply desired heat fluxes, the heater was connected to the power supply unit. The electric current and voltage were stabilized and measured with an accuracy of 0.01 A and 0.1 V, respectively.

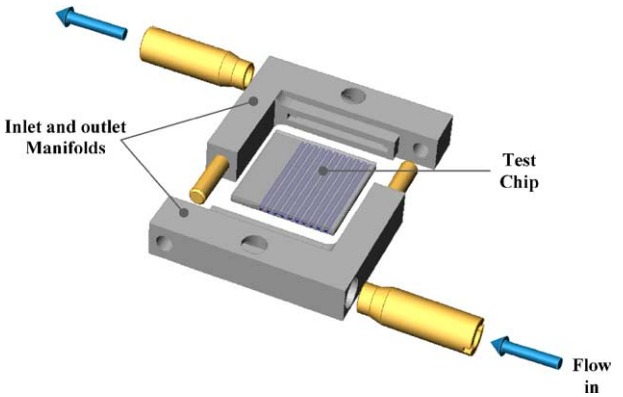

Fig. 2. Test module system.

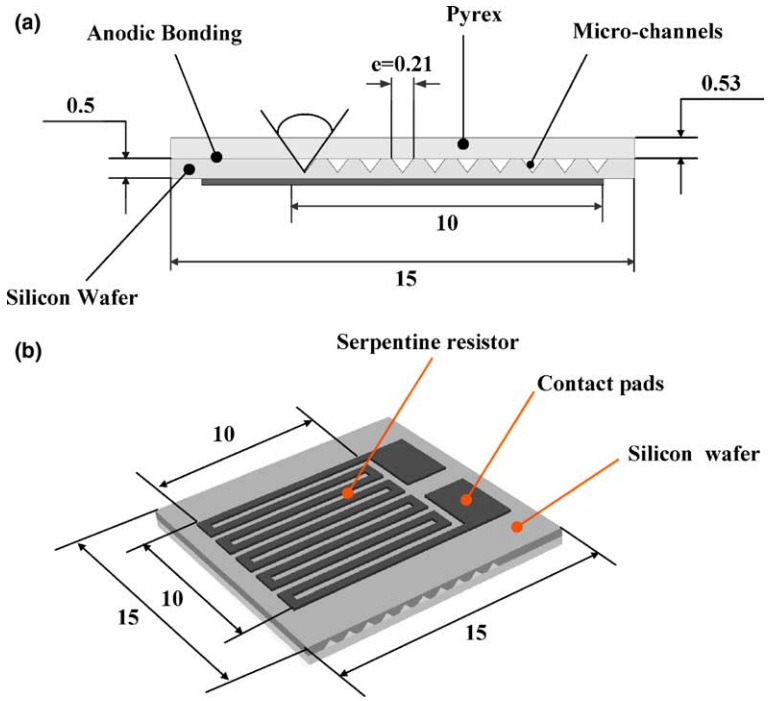

Fig. 3. Test chip with heater. (a) Cross-section; (b) heater (all dimensions are in mm).

2.3. Measurement systems

The temperature of the working fluid was measured at the entrance and exit of the test module by 0.3 mm T-type thermocouples with an accuracy of 0.5 °C. The thermocouples were calibrated at an increment of 0.1 °C using a standard calibration table. The inlet and the outlet of the test section were connected to junctions made of glass. The tip of the thermocouple was placed on the axis of the junction. The thermocouple was insulated from the walls of the junction and we measured the temperature of the liquid or liquid–steam mixture. Pressures were measured, at the inlet and the outlet of the micro-heat sink using pressure transducers. The transducer output voltage was linearly calibrated to kPa units. The data were collected by a digital data collecting system. The overall accuracy of the system was ±0.1% of the input signal for the pressure transducers and of ±1.2 °C for T-type thermocouples with 0.3 °C increments. A sensitive rotameter with an accuracy of 2% was used to measure and control the fluid flow rate. The rotameter was separately calibrated for each type of fluid that was pumped through the experimental system.

2.4. Infrared radiometer

To study the temperature field of the resistor that simulated the heat produced by the electronic transistors, a high-speed focal plane array radiometer containing 75 kpixels was utilized. The measurement resolution was of 0.03 °C with a standard measurement accuracy of ±2 °C for the range

of 0–100 °C and of ±2% above 100 °C. In an isolated laboratory environment using an appropriate black body, improved calibration and non-uniformity-correction are possible; therefore an accuracy of ±1 °C could be achieved. Using a microscopic lens and a reduced array size, IR measurements can be taken up to 800 Hz with a 30 μm spatial resolution. The heater was coated with a thin layer of black diffusive paint, with an emission coefficient of $\varepsilon \approx 0.96$. The determination of the emission coefficient was conducted through the method described in detail by Hetsroni et al. (2003).

2.5. Flow visualization apparatus

A microscope with a zoom ability up to 40× was connected to an external lighting arrangement. An additional camera joint was assembled to connect a high-speed camera to the microscope. The high-speed camera with a maximum frame rate of 10,000 fps, was used to visualize the two-phase flow regimes in the micro-channels. Care was taken to minimize the thermal effects due to illuminating light. The test module was properly shielded from the illuminating light except for the tested micro-channels. The filter between the light source and the micro-channels was placed to reduce the thermal radiation, and the illumination time was reduced to a minimum (about 5 s) to prevent heating of the module. The flow pattern images were obtained at a spatial resolution of 5.3 μm. The frame rate ranged from 250 to 1000 fps, depending on the heat flux and mass flow rate.

2.6. Surfactant properties

The surfactant used in the present study was of the alkyl poly glycosides (APG) type. They are non-ionic surfactants, which are not toxic, especially in minute quantities. Only at high concentrations, they have to be considered as irritating to the skin and eyes (Karlheinz et al., 1996). During the production procedure of medium and long APGs chains, the insoluble dodecanol and tetradecanol chains are chemically treated to create water-soluble surfactants. Fig. 4 shows the dependence of shear viscosity of APG solutions for different mass concentrations, on shear rate at the temperature $T = 60$ °C. A non-Newtonian fluid behavior is revealed for surfactant solution concentrations of up to 600 ppm.

Karlheinz et al. (1996) attribute the difference in shear rate for APG surfactants in comparison to water, to steric hindrances during the shearing of rod-like micelles, which are formed even at very low concentrations and overlap one another in space.

Fig. 5 shows the effect of APG additives on the dynamic and the static surface tension for different mass concentrations, measured at 75 and 95 °C. The dashed lines represent the surface tension value for pure water at 75 °C and 95 °C. Solid points represent the APG data at 75 °C and the hollow points represent the APG data at 95 °C. Note that an increase in concentration decreases surface tension down to a value of 31 mN/m, compared to 59.9 mN/m for pure water.

As in the case reported by Karlheinz et al. (1996) for titanium oxide surfaces, the adsorption of non-ionic surfactants to silicon oxide (silica) surfaces is believed to occur due to the hydrogen bonding of the APG hydroxyl groups with the oxygen atoms of the silicon oxide surface. In continuance, molecules of APG are further adsorbed one to another due to interaction of alkyl chains.

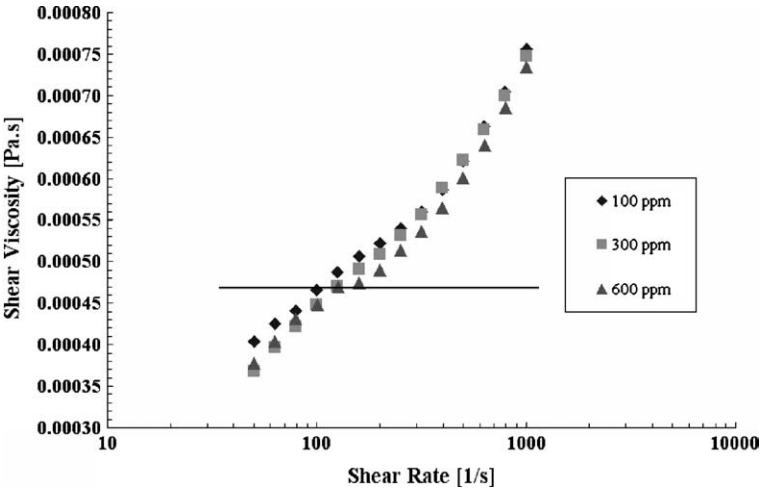

Fig. 4. Shear viscosity of APG surfactant solutions at 60 °C. (By permission Y. Zhang and J.L. Zakin).

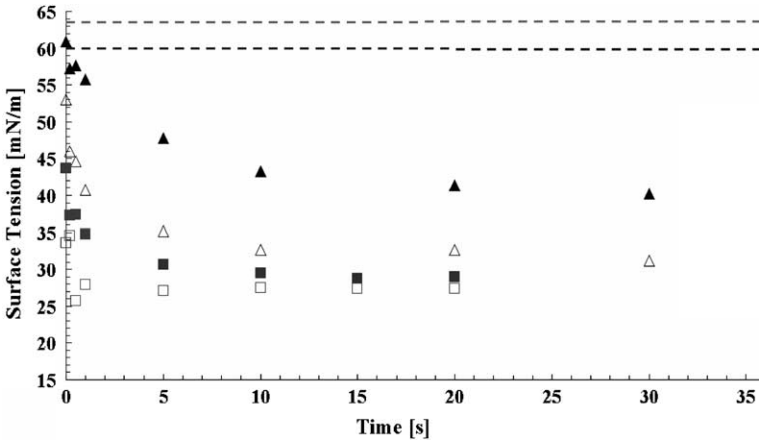

Fig. 5. Surface tension of the APG solutions. Concentration and solution temperature (°C): $C = 100$ ppm—▲ 75, △ 95; $C = 300$ ppm—■ 75, □ 95. (By permission Y. Zhang and J.L. Zakin).

3. Experimental procedure

The experiments were performed using de-ionized water and surfactant solutions. Proper stirring and heating of the de-ionized water with minute amounts of 50% concentrated APG surfactant produced the required solution. In continuation, the solution was diluted to create 100–300 ppm surfactant solutions, to be used in the experiments.

The working liquid was pumped through the test module at relatively low mass fluxes varying from 39 to 173 kg/m^2 s and the applied heat flux was varied from 1 to 50 W/cm^2. At low mass fluxes combined with low heat fluxes, steady state conditions were achieved within 15–30 min. For high heat fluxes, at which two-phase steam–liquid flow took place, the time to achieve the

steady state was less than 5 min. For the normal testing procedure, the pump was turned on, the flow rate and the electric power to the heater were adjusted to a desired level and the temperatures were measured at steady state conditions.

4. Results and analysis

The fluid was pumped from the entrance tank towards the tested MCHS module. As the flow progressed, it first passed through the inlet manifold of a 4 mm inner diameter. Due to relatively high axially conducted heat, fluid pre-warming occurred within the inlet manifold and additional warming occurred within the outlet manifold. Furthermore, as shown in Fig. 6, because of the particular manifold design and pressure drops an uneven liquid distribution in the parallel micro-channels can be observed. The arrows in Fig. 6 illustrate the velocity decrease of the entering fluid, in the longitudinal direction. For single-phase flow, under constant and uniform heat flux conditions, different velocity distribution leads to spanwise temperature gradients. Fig. 7a and c shows a typical temperature field on the heater using single-phase flow. The fluid flows from the top to the bottom, the heat flux is $q_{on} = 16.2$ W/cm^2 and the mass flux is $\dot{m} = 116.2$ kg/m^2 s. In this figure, the arrows qualitatively show the inlet and outlet velocities through various micro-channels and the square marked region of 10×10 mm shows the heated area to which we restricted the thermal image analysis. Fig. 7b shows the temperature distribution along lines 1, 2 and 3 marked in Fig. 7a. We also measured the temperature distribution in the flow direction (Fig. 7d) along lines 4 and 5 shown in Fig. 7c. Fig. 7e shows the measured temperature histogram for which a mean temperature of 79.5 °C and a standard deviation of 12.7 °C were calculated. The heat losses due to conduction, convection and radiation, as estimated for each flow regime, were in the range of 10–17%, depending on the flow rate and heat flux. For example, at mass flux $\dot{m} = 84.9$ kg/m^2 s, heat flux $q_{on} \approx 9.9$ W/cm^2 the heat losses from the Pyrex cover were 1%, from the heater 1.2%, from the inlet manifold 3%, from the outlet manifold 11%. Fig. 8 shows a typical heater temperature map for two-phase surfactant solution boiling flow. At a mass flux of $\dot{m} = 57.2$ kg/m^2 s and heat flux $q_{on} \approx 24.3$ W/cm^2 a mean temperature of 105.6 °C was measured and a standard deviation of 2.9 °C was calculated. Note the relatively small temperature gradient

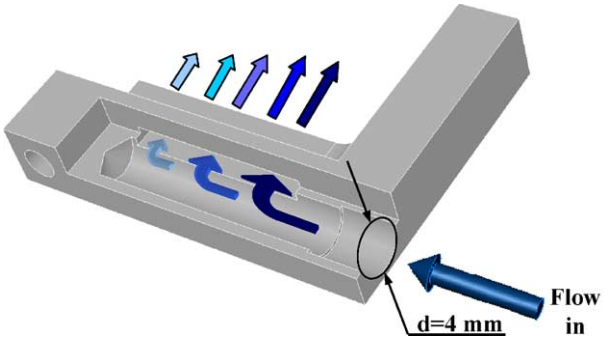

Fig. 6. Schematic of the flow in the inlet manifold.

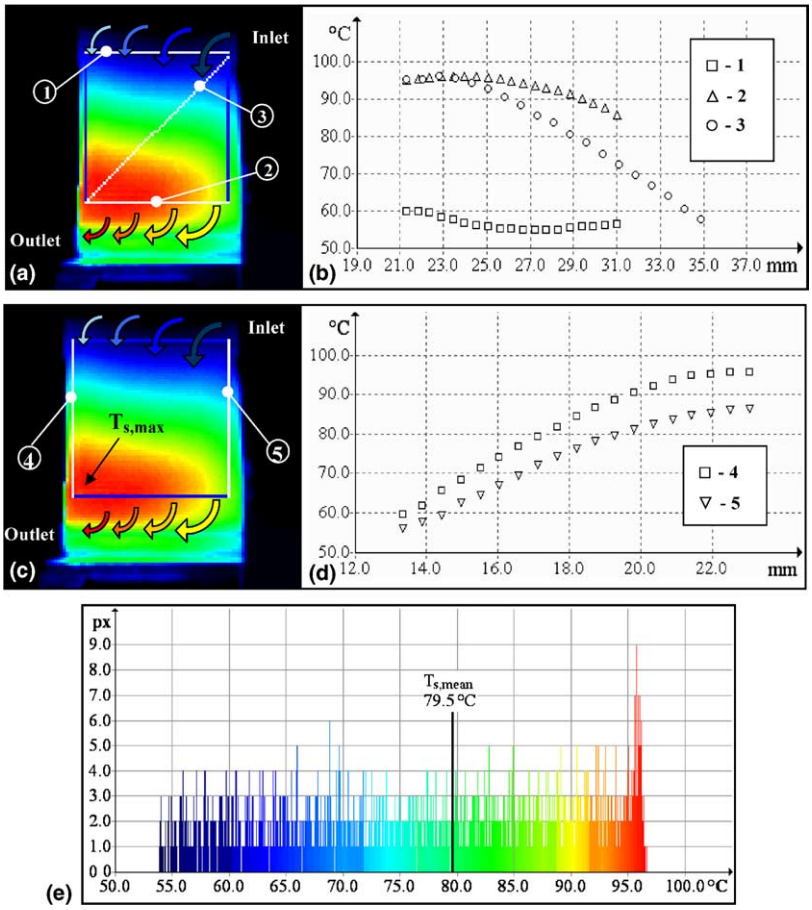

Fig. 7. Typical temperature field, profiles and histogram of the heater surface for single-phase flows.

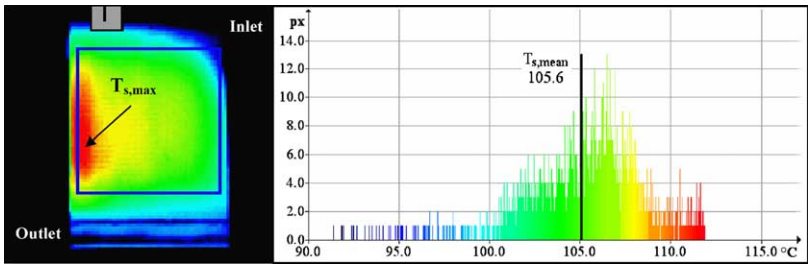

Fig. 8. Typical temperature field and histogram of the heater surface for two-phase flows.

in Fig. 8 compared to the one observed in Fig. 7. At the last stage of the flow, the outlet manifold funnelled the fluid to the outlet tubing, into the exit accumulation tank.

4.1. Single-phase flow

In Fig. 9 and Table 1, the maximum temperatures on the heater, $T_{s,max}$, are presented versus the applied heat flux, q_{on}, for single-phase de-ionized water and 100 ppm APG surfactant solution flows. The solid points in Fig. 9 (including ⊠ marks) connected by continuous lines represent the data for de-ionized water and the hollow (including ⊠ marks) points connected by dashed lines represent the data for 100 ppm APG surfactant solution. The experiments were conducted at various mass fluxes, $\dot{m}$, which were calculated for the micro-channel array cross-section that included 26 micro-channels of a 108 μm hydraulic diameter each. For both water and surfactant solution, at given values of mass flux, the maximum temperature on the heater increased linearly with increasing heat flux. For both water and surfactant solution, $T_{s,max}$ was almost the same. In contrast to turbulent flows in macro-tubes (Aguliar et al., 1999), the APG surfactant additives do not seem to affect the heat transfer.

Table 1 shows a comparison between maximum heater temperature at the initiation of two-phase flows for de-ionized water and 100 ppm APG solution. The initiation of two-phase flows was visually detected and the measurement of the temperatures at the heater was performed

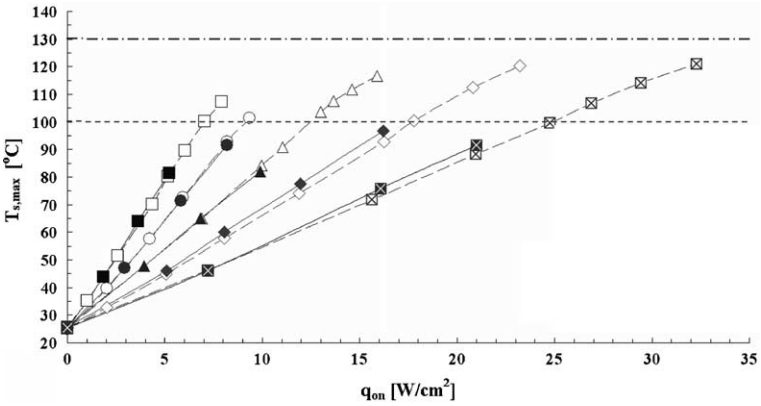

Fig. 9. Dependence of maximum heater temperature on the heat flux for single-phase flows. De-ionized water—■ 37.9, ● 57.7, ▲ 84.9, ◆ 116.2, ⊠ 172.3. APG solution—□ 39.4, ○ 57.2, △ 83.3, ◇ 117.6, ⊠ 171.2 (kg/m^2 s).

Table 1
A comparison between maximum heater temperature at the initiation of two-phase flow of de-ionized water and 100 ppm APG solution flows

De-ionized water			APG-100 ppm, surfactant solution		
Mass flux (kg/m^2 s)	q_{on} (W/cm^2)	$T_{s,max}$ (°C)	Mass flux (kg/m^2 s)	q_{on} (W/cm^2)	$T_{s,max}$ (°C)
37.9	5.2	81.6	39.4	7.7	107.3
57.7	8.2	91.6	57.2	9.3	101.4
84.9	9.9	81.9	83.3	15.9	116.6
116.2	16.2	96.6	117.6	23.2	120.3
172.3	21.0	91.6	171.2	32.3	121.1

simultaneously. As can be seen in Table 1, APG solution single phase is maintained until significantly higher surface temperatures are reached.

4.2. Two-phase flow

The solubility of dissolved gases in liquids decreases with an increase in the liquid temperature. This causes a release of dissolved gases as the liquid temperature is raised, resulting in an early heterogeneous nucleation at temperatures levels well below the saturation temperature. The effect of secluded nucleation and motion of bubbles due to dissolved gases seems to disappear quickly at higher temperatures as fully developed boiling conditions are approached. The experimental observations show that the premature two-phase flow structure in de-ionized water flows does not occur in all micro-channels, but rather at locations that exceed surface temperatures of 80 °C, because in these channels the velocity of the liquid is low. This phenomenon was observed by Zhang et al. (2002a) in experiments on water flowing through a 113 μm hydraulic diameter micro-channel and also for water flows in macro-tubes as mentioned by Kandlikar and Bulut (2003). An experimental investigation was performed by Steinke and Kandlikar (2004) to study the control of dissolved gases and their effect on heat transfer and pressure drop during the flow of water in six parallel micro-channels of a 200 μm hydraulic diameter and a 57.15 mm length. It was shown that beyond a certain heat flux and surface temperature, fully developed boiling ensues and all heat transfer coefficients for different dissolved gas cases collapse to a single curve.

Typical images of nucleation activity in the presence of dissolved gases (small separated and elongated bubbles in water flows) are shown in Fig. 10a–c. The flow moved from the top to the bottom, and the field of view is 1.3×1.0 mm. The heat flux in Fig. 10a is $q_{on} = 7.5$ W/cm^2 and the mass flux is $\dot{m} = 80.0$ kg/m^2 s. The heat flux in Fig. 10b and c is $q_{on} = 4.9$ W/cm^2 and the mass flux is $\dot{m} = 58.2$ kg/m^2 s.

At low mass fluxes and moderate heat fluxes, bubbles that originate from desorption of dissolved gases may fill the micro-channels in which they are accumulated. As can be seen in Fig. 9, this phenomenon does not significantly affect the single-phase heat transfer. The behavior may be explained by simultaneous production of a small number of air bubbles in different channels, in response to which, the liquid correlates its flow velocity through the nearby channels. Thus, the linear trend of wall temperature rise at steady state conditions was maintained up to higher surface temperatures.

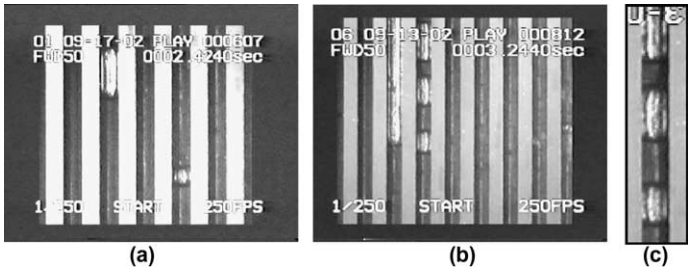

Fig. 10. (a,b) Typical images of nucleation activity in the presence of dissolved gases, (c) is an enlargement of the third micro-channel from the left in (b).

For APG surfactant solution, no gas bubbles were observed. Moreover, the two-phase boiling flow regime was abruptly initiated at heater surface temperatures higher than 120 °C.

Fig. 11 shows the maximum heater temperature versus the applied heat flux for both single- and two-phase flows of water and surfactant solution. The continuous lines connecting the solid points and the dashed lines connecting the hollow points describe the data for water and APG surfactant solution, respectively. The data points marked by a circles represent the maximum heat flux achieved for each value of mass flux. With the intention of obtaining the entire boiling curve, the power applied to the test module was increased by small increments, while the total fluid flow rate through the heat sink was maintained at a constant level. As shown in Fig. 8 presented by Jiang et al. (1999), for increasing power supply, a sharp increase of surface temperatures is expected between 100 and 150 °C. In order to avoid the sharp increase (onset of CHF), resulting in chip burnout, our experiments did not exceed the maximum temperature at the heater of $T_{max} = 130$ °C. It can be seen that at relatively low mass fluxes (up to about 83 kg/m^2 s), the initiation of a two-phase boiling flow significantly decreases the slope of the boiling curve for both water and surfactant solution. The boiling curve plateau may be associated with the saturated boiling state, where bubbles are formed at higher rates and coalesce to form fluctuating annular flows. These flow regimes lead to increased heat transfer coefficients and surface temperature do not increase with increasing power supply until onset of CHF is approached. Similar results were presented by Zhang et al. (2002a) and Lee et al. (2003) for water flow in a 113 and 24 μm hydraulic diameter micro-channels, respectively. Nevertheless, the experiments performed by Jiang et al. (1999, 2001) and Zhang et al. (2002a) did not reveal such a phenomenon for water flow in micro-channels with a hydraulic diameter of 40–80 μm. The plateau was also not observed in the experiments of Zhang et al. (2002a) with Triton X-100 surfactant conducted in the 44 μm hydraulic diameter micro-channel, implying that reduced surface tension does not lead to saturated nucleate boiling in micro-channels. The aforementioned results suggest that the boiling curve plateau may not be solely associated with the hydraulic diameter or static surface tension. Therefore, parameters such as surface materials, surface treatments, surface roughness and dynamic surface tension and contact angle need to be considered as well.

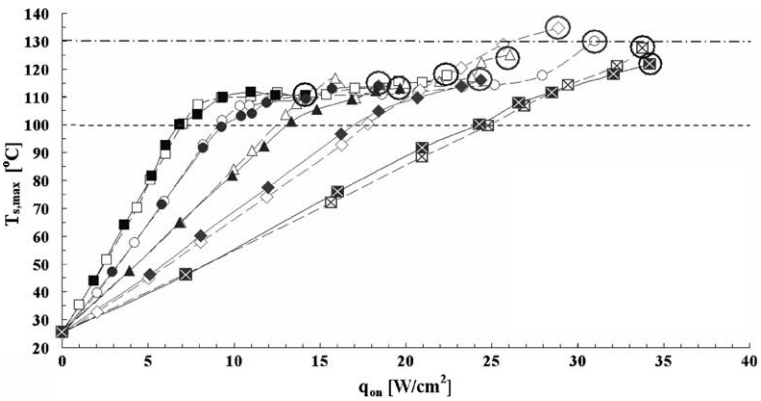

Fig. 11. Dependence of maximum heater temperature on heat flux for single- and two-phase flows. De-ionized water—■ 37.9, ● 57.7, ▲ 84.9, ◆ 116.2, ⊠ 172.3. APG solution—□ 39.4, ○ 57.2, △ 83.3, ◇ 117.6, ⊠ 171.2 (kg/m^2 s).

Moreover, the results brought in this report, as well as other reports found by the authors, agree with Stephan (1992) who stated that for boiling water at 1 bar the critical bubble diameter is on the order of 150 μm. The highest pressure measured in our experiments was about 1.15 bar and even at excess temperatures as high as 30 °C no phase-change bubbles could be observed.

Fig. 11 also shows that among the tested mass fluxes there may be found an optimum value of mass flux that produced maximal increase in the heat removal ability of surfactant in comparison to de-ionized water flow. This optimal flux was about 57 kg/cm^2 s. Table 2 shows the maximum temperature gradients, $\Delta T = T_{max} - T_{min}$, on the heater for water and 100 ppm APG surfactant solution at mass fluxes $\dot{m} = 57$–58 kg/m^2 s and $\dot{m} = 172$–173 kg/m^2 s, respectively. One can see that at $\dot{m} = 57$–58 kg/m^2 s and $q_{on} = 18.4$ W/cm^2 the maximum gradient is $\Delta T = 22.1$ K for water flow. For the surfactant solution, it is 20.5 K at the same mass flux, but at higher heat flux, $q_{on} = 24.3$ W/cm^2 (the temperature map for this case can be seen in Fig. 8). For $\dot{m} = 172$–173 kg/m^2 s, the results are about the same for water and surfactant flows.

Fig. 12 shows boiling curves for two mass fluxes. The continuous lines connecting the solid points and the dashed lines connecting the hollow points describe the data for water and 100 ppm APG surfactant solution, respectively. Arrows in Fig. 12 emphasize the onset of CHF (Bowers and Mudawar, 1994). This figure shows that for boiling flow of water at mass flux $\dot{m} = 57$–58 kg/m^2 s and heat flux $q = 18$ W/cm^2, the mean temperature on the heater is $T_{mean} = 110$ °C. For flow boiling of the surfactant and the same mean temperature at the heater,

Table 2
Overall heater temperature gradients for two-phase de-ionized water and 100 ppm APG surfactant solution flows

De-ionized water			APG 100 ppm solution		
Mass flux (kg/m^2 s)	q_{on} (W/cm^2)	ΔT (K)	Mass flux (kg/m^2 s)	q_{on} (W/cm^2)	ΔT (K)
57.7	18.4	22.1	57.2	24.3	20.5
172.3	32.1	59.5	171.2	32.3	59.9

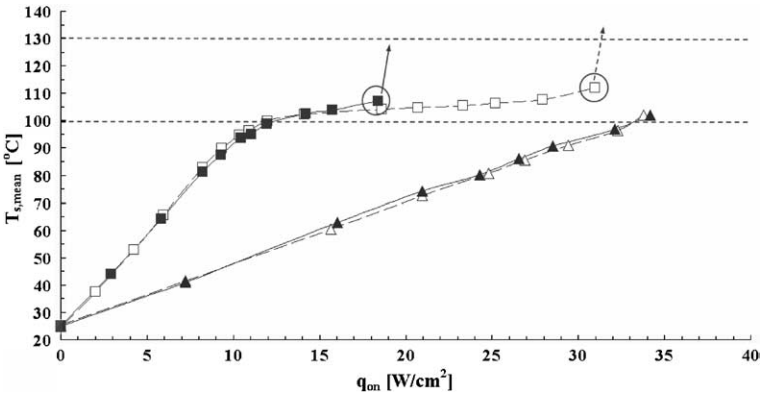

Fig. 12. Dependence of the mean heater temperature on heat flux for single- and two-phase flows. De-ionized water—■ 57.7, ▲ 172.3. APG solution—□ 57.2, △ 171.2 (kg/m^2 s).

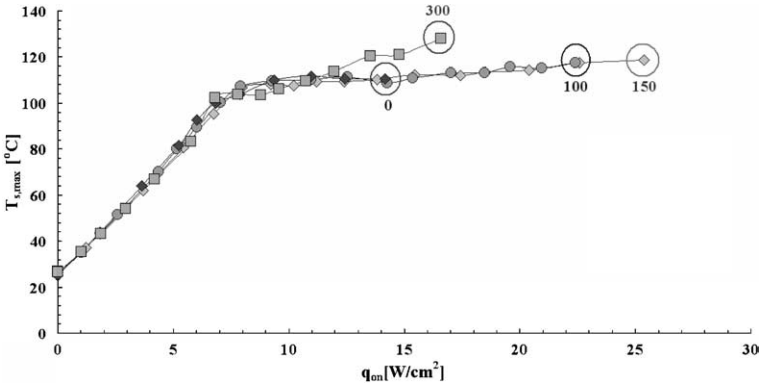

Fig. 13. Effect of solution concentration on the boiling curve. APG solution—♦ 37.9, 0; ● 39.4, 100; ◇ 37.9, 150; ■ 39.7, 300 (kg/m^2 s, ppm).

the heat flux is $q = 28$ W/cm^2, that is, the heat transfer coefficient increases about 1.6-fold. This effect vanishes at mass flux $\dot{m} = 172$–173 kg/m^2 s as does the onset of CHF.

Fig. 13 shows a comparison between five various experiments conducted with surfactant solutions at different concentrations. The mass flux, $\dot{m}$, was about 38 kg/m^2 s. The continuous lines connecting the '◆', '●', '◇' and '■' points represent experiments performed using de-ionized water (0 ppm), and 100, 150 and 300 ppm surfactant solutions, respectively. It can be observed that the use of 150 ppm surfactant solution flow yields the best results compared to de-ionized water flow. The maximum heat flux for the 300 ppm surfactant solution is less than that for the 150 ppm solution. These results show that there is an optimal of surfactant solution concentration that causes a considerable increase in two-phase flow heat transfer.

Fig. 14 shows the mean temperature on the heater, $T_{s,mean}$, versus the applied power. The results obtained by Jiang et al. (2002) and Wang et al. (2002) for experimental data of an array

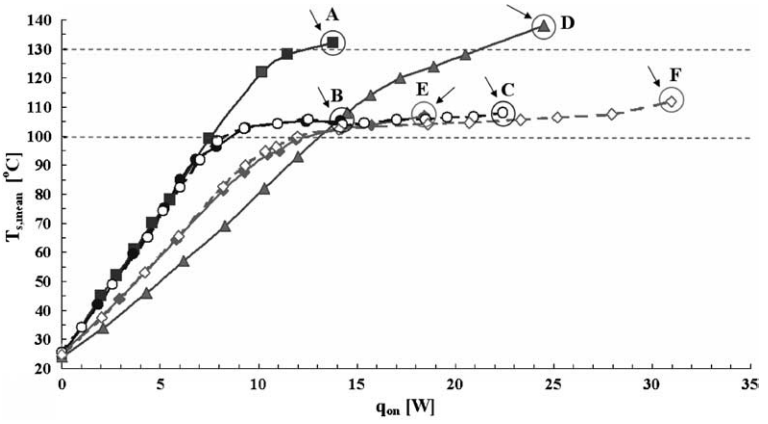

Fig. 14. Dependence of heater mean temperature on applied power. (■) A—water, Jiang et al. (2002), 41.5 (kg/m^{2}s); (●) B—water present results, 37.9 (kg/m^{2}s); (○) C—APG solution, present results, 39.4 (kg/m^{2}s). (▲) D—water, Jiang et al. (2002), 83.1 (kg/m^{2}s); (♦) E—water, present results, 57.7 (kg/m^{2}s); (◊) F—APG solution, present results, 57.2 (kg/m^{2}s).

of 40 silicon-etched micro-channels, with a hydraulic diameter of about 100 μm are also shown for comparison. The comparison shows that in the present study the maximum heat fluxes removed by water and surfactant solutions were higher than those reported by Jiang et al. (2002). Note that at about the same value of mass flux, the average surface temperature in the present study was significantly lower than that reported by Jiang et al. (2002).

4.3. Two-phase flow regimes

The bubble growth mechanism seems to be restricted by the channel size. For water flows, with dissolved gases, the two-phase flow regime begins at about 80 °C, because of air accumulation and release in some nucleation sites. If the liquid mass flux is relatively high, the bubble slides along the surface of the micro-channel and does not fill up the channel. Finally, the bubble moves with the bulk flow. A non-dimensional parameter $q^* = q_{on}/\dot{m}_{tot}h_{LG}$, where q_{on} is heat flux, $\dot{m}$ is mass flux and h_{LG} is latent heat of vaporization, denotes the ratio between the applied heat flux to the maximum possible removable heat by a phase change at a given mass flux. Fig. 15 shows a simple two-phase flow regime map determined by flow visualization for the presently studied MCHS. The Re_{in} parameter is based on the inner diameter of the manifold and flow velocity in the inner manifold. For relatively low values of q^*, the removed bubbles are of a small diameter; therefore, the overall flow disturbance is not meaningful. This kind of flow is characterized as Bubbly flow:single (SBF), rapid (RBF) and multiple rapid bubble flow (MRBF)—see Fig. 10. At medium values of q^*, the surface temperatures rise above the saturation value at the local pressure, and the bubbles created are the result of a phase change. The bubbles are now produced at an increased rate and size and, therefore may partially fill the micro-channel volume. At this flow regime, the fluid flow pressure is equal or higher than the local pressure generated within the channels; therefore, a fluctuating two-phase interface is observed—see Fig. 16, arrow a. Fig. 16 was obtained under a heat flux of 5.7 W/cm^2 at a 46.7 kg/m^2 s mass flux. The black color inside the channel in these figures represents the water phase and the white color represents vapor phase. The flow regime shown in Fig. 16 (arrow a) is characterized as quasi-stable flow (QSF). When vapor fills nearly the whole micro-channel, the flow is characterized as partial unsteady annular

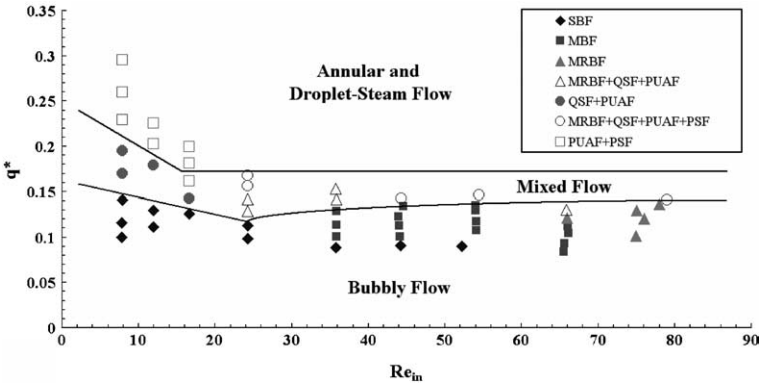

Fig. 15. Two-phase flow regime map.

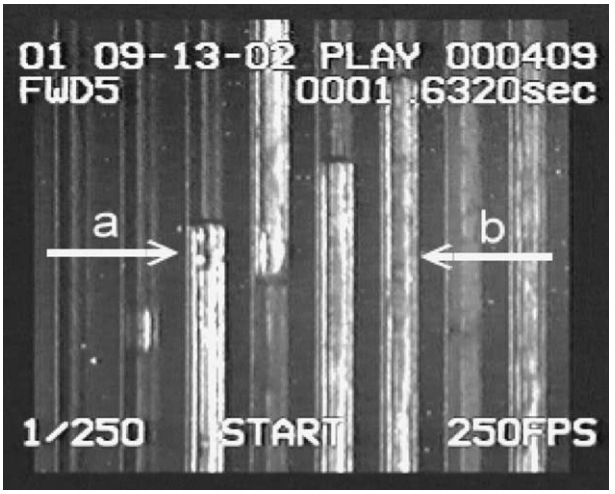

Fig. 16. Typical two-phase flows taken by the high-speed camera. Arrows a and b show respectively QSF and PUAF flow regimes.

flow (PUAF) and shown in Fig. 16 (arrow b). In this flow regime, a thin liquid film is always present on the micro-channel surfaces. The "Partial" expression refers to the nature of the fluctuating regime. Fig. 17 was obtained under a heat flux of 15.5 W/cm^2 at a 116.5 kg/m^2 s mass flux. In these figures, the black color inside the channels represents moving vapor flow and the white color represents an evaporating water phase. The difference between the colors associated with the fluid and vapor phases in Figs. 16 and 17 is due to different illumination directions. At the highest values of q^*, the flow regime is characterized as partial steam or droplet-steam flow (PSF). In this

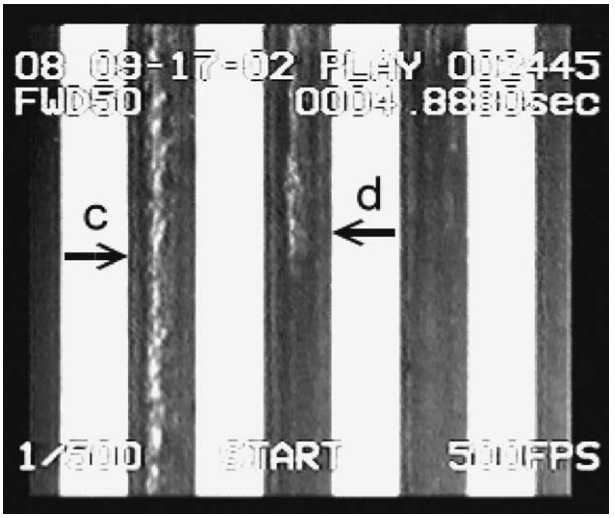

Fig. 17. Partial steam flow regime image taken by the high-speed camera. Arrows c and d show PSF flow regime.

flow regime, the vapor phase is in contact with the micro-channel surface while the liquid phase can usually be observed evaporating at the center of the micro-channel, as could be seen in Fig. 17 (arrows c and d). If at this point the channels are kept long enough without water, due to a massive phase change activity in a large number of micro-channels, the heat transfer coefficient decreases considerably resulting in a sharp temperature rise—CHF. The two-phase flow regimes discussed in the present study are in general agreement with the observations reported by Zhang et al. (2002a) and Qu and Mudawar (2002c).

It should be noted that because of the ill-distributed flow between the different micro-channels, various flow regimes co-existed in different channels. Therefore, the overall flow regime map in Fig. 15 for this specific MCHS could be divided into three parts—bubbly flow, mixed flow (including rapid bubbly and quasi-stable flows) and annular/droplet-steam flow.

In contrast to water flow, the two-phase flow regime using surfactant solution flow is initiated at higher surface temperatures. The addition of small amounts of surfactants changes the fluid two-phase flow regimes by eliminating the bubbly regime and abruptly beginning the two-phase flow regimes at moderate to high heat fluxes. No other meaningful difference in flow regimes was observed.

5. Discussion

In order to elucidate the boiling characteristics of water with surfactant additives, several different mechanisms have been postulated in the literature. These have focused on the role of additives in altering interfacial properties of the solution, including equilibrium surface tension, dynamic surface tension, Marangoni convection, and the surfactant's ionic nature and molecular weight.

5.1. Effect of surfactants on boiling enhancement

Wasekar and Manglik (2002) presented the results of a study that investigates the dependence of nucleate boiling heat transfer coefficients of aqueous surfactant solutions on the additives' molecular weight and ionic nature. Two anionic (SDS and SLES) and two non-ionic (Triton X-100 and Triton X-305) surfactants were used in various concentrations. The boiling performance, characterized by an early onset of nucleate boiling, was significantly enhanced, and the maximum enhancement increased with decreasing surfactant molecular weight, M. The heat transfer coefficient, normalized by dynamic surface tension, h^*, scales as $h^* \sim M^n$ with $n = -0.5$ and $n = 0$ for anionics and non-ionics, respectively. It should be noted that the dependence $h^* \sim M^n$ was determined only for the four surfactants considered by Wasekar and Manglik (2002).

Criteria for nucleate boiling enhancement by surfactant additives were proposed by Yang and Maa (2003). As the first criterion, it was postulated that the surfactant should be soluble in water. As the second criterion, it was postulated that the surfactant should depress the equilibrium surface tension of water significantly. As the third criterion, it was postulated that the surfactant should not depress the equilibrium contact angle significantly. According to Yang and Maa (2003), boiling heat transfer by addition of a surfactant is enhanced by the depression of the equilibrium surface tension but suppressed by the depression of the equilibrium contact angle.

Sher and Hetsroni (2002) developed a model of nucleate pool boiling with surfactant additives. Solid–vapor, solid–liquid and liquid–vapor surface tensions were postulated to be surfactant diffusion controlled, and expressions for them were derived. Using these expressions the boiling curve was obtained as a function of surfactant bulk concentration. The model was compared to experimental boiling curves obtained by Hetsroni et al. (2001a,b) for pool boiling of cationic surfactant. Comparison between theoretical and experimental results shows a good agreement.

By using thermodynamic considerations, Carey (1992) showed that by lowering the surface tension of a liquid in contact with a solid surface, the number of active heterogeneous nucleation sites is raised, the nucleation rate is increased and the bubble size is reduced. It is believed that this combination increases the heat removal ability by amplifying liquid phase change. Consequently, as can be observed in Figs. 10–12, the use of surfactant solution, has kept surface temperature at a nearly constant level over a wide range of applied heat fluxes. This phenomenon could be compared to the effect of "enhanced surface" as reported by Zhang et al. (2002a).

The present study shows that under conditions of boiling flow at low mass fluxes addition of surfactants leads to an increase in heat transfer compared to that of water. This phenomenon may be explained using Yang and Maa (2003), Sher and Hetsroni (2002) or Carey (1992) models. However, with increasing flow velocity, a large velocity difference between the two phases serves to destabilize the interface. In this case the body force plays a more important role than surface tension and at the same mass flux heat transfer for surfactant solutions does not differ from that of water.

5.2. Effect of surfactant concentration on the heat transfer

The influence of surface tension on boiling heat transfer is neither simple nor direct. The surface tension of a rapidly extending interface in surfactant solution may be different from the static value, because the surfactant component cannot diffuse to the absorber promptly. This may result in an interfacial flow driven by the surface tension gradient $\Delta\sigma$ (known as the Marangoni flow). The effect of surfactant concentration on the Marangoni convection around vapor bubbles has been numerically investigated by Wasekar and Manglik (2001). The model consists of an adiabatic, rigid, hemispherical bubble on a downward facing constant temperature heated wall, in a fluid pool with an initial uniform temperature gradient. It was shown that the resulting concentration gradients promote flows, which act in the same direction as temperature gradient induced flows, thereby enhancing the convection significantly. Flow boiling experiments in aqueous surfactant solutions of concentration $C = 300$ ppm conducted in the present study did not show heat transfer enhancement compared to those of concentration $C = 100$ ppm. In order that this result can be explained, other heat transfer mechanisms should be proposed for boiling in surfactant solutions.

We consider a fluid zone of thickness d across which the surface tension difference is $\Delta\sigma$. The Marangoni number $Ma = \Delta\sigma d/\rho v k$ is the parameter that affects the heat transfer (where ρ is the density, v is the kinematic viscosity and k is the thermal diffusivity of the solution). The Marangoni number can be read as boiling heat transfer by addition of a surfactant and is enhanced by the depression of equilibrium tension, σ, but suppressed by the increasing kinematic viscosity, v. These two effects counterbalance each other depending on the concentration and result in different degrees of boiling enhancement.

From the physical and engineering design point of view, it is desirable that surfactant effects on boiling heat transfer can be generalized. At present, however, only tentative criteria for a given surfactant are available. We are still far from a systematic theory on the enhancement of boiling heat transfer caused by surfactant additives.

5.3. Effect of surfactant adsorbance on surfaces on the boiling process

The dissolved molecules of the surfactant solution are responsible for the lowering of surface tension, by being adsorbed on the phase-change interface. However, by hydrogen bonding of the APG hydroxyl groups with the oxygen atoms of the silicon oxide surface, as in the case reported by Karlheinz et al. (1996) for titanium oxide surfaces, the molecules are adsorbed on the micro-channel surfaces, forming a thin layer. This layer is believed to firmly cover nucleation sites; therefore, direct liquid–surface contact is not possible. As a result relatively elevated heat fluxes over the surface are removed through the surfactant thin layer by single-phase convection, until the layer breaks down. The described phenomenon effect is observed by the absence of a nucleate boiling mechanism until elevated surface temperatures are reached as shown in Table 1 and Fig. 8, for surfactant solution flows. This effect may be positively exploited in micro-channel heat sinks, when the boiling process is not desired because of hydraulic instabilities. With the breakdown of a surfactant layer, the liquid contact at nucleation sites is made possible and the initiation of boiling regime is abrupt. A careful observation of the boiling process inside the outlet collector revealed that the boiling process has begun inside the outlet collector even though it was not observed within the micro-channels. These observations lead us to conclude that contrary to the micro-channels surfaces, the manifolds' inner surface was not covered in the same way by the surfactant molecules. It is believed that the surfactant absorbance to a non-polished metal surface is of a different nature than that of a silica-covered surface; therefore, nucleation sites were activated at different temperatures/heat fluxes on the inner face of the outlet collector.

6. Conclusions

The study was focused on the effects of APG surfactants on heat transfer of a single-phase and boiling flows in micro-channels. The results were compared to heat transfer in water flow under similar conditions. For single-phase flow, no significant difference was observed between heat transfer in water and surfactant solutions at various mass concentrations. It was shown that water flows with dissolved gasses might induce premature nucleation processes at surface temperatures as low as 80 °C. However, the introduction of surfactants to water eliminates the separated bubble flow regimes. Single-phase flows were observed at elevated surface temperatures (as high as 120 °C), at which quasi-stable boiling flow was abruptly initiated. This effect may be associated with the adsorbance of surfactant molecules to the silica surfaces of the micro-channels.

For boiling flow of surfactant solutions, the optimal value of mass flux was found at which the heat transfer enhancement reached its maximum. The experiments have also revealed that at low mass fluxes, an optimal mass concentration of APG additives may be found, for which a two-phase flow heat transfer significantly increases. The phenomenon may be connected to the Marangoni effect.

These findings lead to the conclusion that the use of surfactants should be considered as a method for improving two-phase boiling flow heat transfer. Further effort should also be invested on revealing proper surfactant additives and performing experiments of surfactant solutions flowing through a various micro-channel heat-sink configurations.

Acknowledgments

This research was supported by the Fund for the Promotion of Research at the Technion and by the OPTIPAC consortium. A. Mosyak is supported by a joint grant from the Center for Absorption in Science of the Ministry of Immigrant Absorption and the Committee for Planning and Budgeting of the Council for Higher Education under the framework of the KAMEA program. The authors are indebted to Prof. J.L. Zakin, Jeffrey Ellis and Ying Zhang who performed the measurements of surfactant properties at the Ohio State University. Finally, the authors would like to thank Jacob Leemaster and Sergio Malamut for their contribution to this research.

References

Aguliar, G., Gasljevic, K., Matthys, E.F., 1999. Coupling between heat and momentum transfer mechanism for drag-reducing polymer and surfactant solutions. J. Heat Transfer 121, 796–802.

Bowers, M.B., Mudawar, I., 1994. High flux boiling in low flow rate, low pressure drop mini-channel and micro-channel heat sinks. Int. J. Heat Mass Transfer 37, 321–332.

Carey, V.P., 1992. Liquid Vapor Phase-change Phenomena. Hemisphere Publishing Corporation.

Choi, S.B., Barren, R.R., Warrington, R.Q., 1991. Fluid flow and heat transfer in microtubes. ASME DSC 40, 89–93.

Gad-el-Hak, M., 1999. The fluid mechanics of micro-devices. The Freemen Scholar Lecture. J. Fluid Eng. 121, 5–33.

Hetsroni, G., Mosyak, A., Segal, Z., 2001a. Nonuniform temperature distribution in electronic devices cooled by flow in parallel micro-channels. IEEE Trans. Compon. Packag. Technol. 24, 16–23.

Hetsroni, G., Zakin, J.L., Lin, Z., Mosyak, A., Pancallo, E.A., Rozenblit, R., 2001b. The effect of surfactants on bubble growth, wall thermal patterns and heat transfer in pool boiling. Int. J. Heat Mass Transfer 44, 485–497.

Hetsroni, G., Mosyak, A., Segal, Z., Ziskind, G., 2002a. A uniform temperature heat sink for cooling of electronic devices. Int. J. Heat Mass Transfer 45, 3275–3286.

Hetsroni, G., Gurevich, M., Mosyak, A., Rozenblit, R., Yarin, L.P., 2002b. Subcooled boiling of surfactant solutions. Int. J. Multiphase Flow 28, 347–361.

Hetsroni, G., Gurevich, M., Mosyak, A., Rozenblit, R., 2003. Surface temperature measurement of a heated capillary tube by means of an infrared technique. Meas. Sci. Technol. 14, 807–814.

Jiang, L., Wong, M., Zohar, Y., 1999. Phase change in microchannel heat sinks with integrated temperature sensors. J. Micro-Electromech. Syst. 8, 358–365.

Jiang, L., Wong, M., Zohar, Y., 2001. Forced convection boiling in a microchannel heat sink. J. Micro-Electromech. Syst. 10, 80–87.

Jiang, L., Koo, J.-M., Zhang, L., Wang, E., Im, S., Yao, S., Zeng, S., Bari, A., Santiago, J.G., Kenny, T.W., Goodson, K.E., 2002. Progress on two-phase convection in microchannel heat sinks. The 4th Pacific Rim Thermal Science and Energy Engineering Workshop (PaRTSEE-4), Kyoto, Japan, 31 May–2 June.

Kandlikar, S.G., 2002. Fundamental issues related to flow boiling in minichannels and micro-channels. Exp. Therm. Fluid Sci. 26, 389–407.

Kandlikar, S.G., Bulut, M., 2003. An experimental investigation of flow boiling of ethylene–glykol/water mixtures. J. Heat Transfer, ASME 125, 317–325.

Karlheinz, H., von Rybinski, W., Stoll, G., 1996. Alkyl Polyglycosides Technology, Properties and Applications. VSH Publishers Inc., New York, NY (USA).

Lee, M., Wong, Y.Y., Wong, M., Zohar, Y., 2003. Size and shape effects on two-phase flow patterns in microchannel forced convection boiling. J. Micromech. Microeng. 13, 1–9.

Mehendale, S.S., Jacobi, A.M., Shah R.K., 1999. Heat exchangers at micro- and mesoscales. In: Proc. Int. Conf. Compact Heat Exchangers and Enhance Technology for the Process Industries, Banff, Canada, pp. 55–74.

Palm, R., 2001. Heat transfer in micro-channels. Microscale Thermophys. Eng. 5, 155–175.

Peng, X.F., Wang, B.X., 1993. Forced convection and flow boiling heat transfer for liquid flowing through microchannels. Int. J. Heat Mass Transfer 36, 3421–3427.

Peng, X.F., Peterson, G.P., 1995. The effect of thermo-fluid and geometric parameters on convection of liquid through rectangular micro-channels. Int. J. Heat Mass Transfer 38, 755–758.

Peng, X.F., Hu, H.Y., Wang, B.X., 1998. Boiling nucleation during liquid flow in microchannels. Int. J. Heat Mass Transfer 41, 101–106.

Peng, X.F., Wang, B.X., 1998. Forced convection and boiling characteristics in microchannels. In: Proc. 11 IHTC, vol. 1, Kyonji, Korea, 23–28 August, pp. 371–390.

Qu, W., Mudawar, I., 2002a. Experimental and numerical study of pressure drop and heat transfer in a single-phase micro-channel heat sink. Int. J. Heat Mass Transfer 45, 2549–2565.

Qu, W., Mudawar, I., 2002b. Analysis of three-dimensional heat transfer in microchannel heat sinks. Int. J. Heat Mass Transfer 45, 3973–3985.

Qu, W., Mudawar, I., 2002c. Prediction and measurement of incipient boiling heat flux in micro-channel heat sinks. Int. J. Heat Mass Transfer 45, 3933–3945.

Qu, W., Mudawar, I., 2003. Flow boiling heat transfer in two-phase micro-channel heat sinks 1. Experimental investigation and assessment of correlation methods. Int. J. Heat Mass Transfer 46, 2755–2771.

Sher, I., Hetsroni, G., 2002. An analytical model for nucleate pool boiling with surfactant additives. Int. J. Multiphase Flow 28, 699–706.

Sobhan, C.B., Garimella, S.V., 2001. A comparative analysis of studies on heat transfer and fluid flow in microchannels. Microscale Thermophys. Eng. 5, 293–311.

Steinke, M.E., Kandlikar, S.G., 2004. Control and effect of dissolved air in water during flow boiling in micro-channels. Int. J. Heat Mass Transfer 47, 1935.

Stephan, K., 1992. Heat Transfer in Condensation and Boiling. Springer-Verlag, Berlin.

Wang, B.X., Peng, X.F., 1994. Experimental investigation of liquid forced-convection heat transfer through micro-channels. Int. J. Heat Mass Transfer 37, 73–82.

Wang, E.N., Zhang, L., Jiang, L., Koo, J.-M., Goodson, K.E., Kenny, T.W., Maveety, J.G., Sanchez, E.A., 2002. Micromachined jet arrays for liquid impingement cooling of VLSI chips, http://www.mit.edu/afs/athena/org/m/micronanosystems/paper12.pdf and www.nnf.cornell.edu/nnun/2002NNUNpg28.pdf.

Warrier, G.R., Dhir, V.K., Momoda, A., 2002. Heat transfer and pressure drop in narrow rectangular channels. Exp. Therm. Fluid Sci. 26, 53–64.

Wasekar, V.M., Manglik, R.M., 2001. Computation of Marangoni convection at the vapor–liquid interface in aqueous surfactant solutions. In: Bathe, K.J. (Ed.), First MIT Conference on Computational Fluid and Solid Mechanics. Elsevier, pp. 1412–1416.

Wasekar, V.M., Manglik, R.M., 2002. The influence of additive molecular weight and ionic nature on the pool boiling performance of aqueous surfactant solutions. Int. J. Heat Mass Transfer 45, 483–493.

Webb, R.L., Zhang, M., 1998. Heat transfer and friction in small diameter channels. Microscale Thermophys. Eng. 2, 189–202.

Weisberg, A., Bau, H.H., Zemel, J., 1992. Analysis of micro-channels for integrated cooling. Int. J. Heat Mass Transfer 35, 2465–2474.

Wu, P.Y., Little, W.A., 1984. Measurement of the heat transfer characteristics of gas flow in fine channel heat exchangers used for micro-miniature refrigerators. Cryogenics 23, 415–420.

Yang, Y.M., Maa, J.R., 2003. Boiling heat transfer enhancement by surfactant additives. In: Proc. Fifth Int. Conf. Boiling Heat Transfer, ICBHT 2003, Montego Bay, Jamaica, 4–8 May.

Zhang, L., Wang, E.N., Koo, J.M., Jiang, L., Goodson, K.E., Santiago, J.G., Kenny, T.W., 2002a. Enhanced nucleate boiling in microchannels, 15th IEEE MEMS Workshop, Las Vegas, Nevada, USA, 20–24 January.

Zhang, L., Ko, J.M., Jiang, L., 2002b. Measurements and modeling of two-phase flow in micro-channels with nearly constant heat flux boundary conditions. J. Microelectromech. Syst. 11, 12–19.